The gene for the lysosomal protein LAMP3 is a direct target of the transcription factor ATF4

Received for publication, November 13, 2019, and in revised form, April 9, 2020 Published, Papers in Press, April 20, 2020, DOI 10.1074/jbc.RA119.011864

Thomas D. Burton[‡1], Anthony O. Fedele[‡1], Jianling Xie (谢 建凌)[§], Lauren Y. Sandeman[§], and Christopher G. Proud[‡¶2]

From the [§]Cell Signalling and Gene Regulation Group and [‡]Hopwood Centre for Neurobiology, Lifelong Health Theme, South Australian Health and Medical Research Institute (SAHMRI), P. O. Box 11060, Adelaide, South Australia 5001 and the [¶]Department of Molecular and Biomedical Science, School of Biological Sciences, University of Adelaide, Adelaide, South Australia 5005, Australia

Edited by Ronald C. Wek

Autophagy and lysosomal activities play a key role in the cell by initiating and carrying out the degradation of misfolded proteins. Transcription factor EB (TFEB) functions as a master controller of lysosomal biogenesis and function during lysosomal stress, controlling most but, importantly, not all lysosomal genes. Here, we sought to better understand the regulation of lysosomal genes whose expression does not appear to be controlled by TFEB. Sixteen of these genes were screened for transactivation in response to diverse cellular insults. mRNA levels for lysosomal-associated membrane protein 3 (*LAMP3*), a gene that is highly up-regulated in many forms of cancer, including breast and cervical cancers, were significantly increased during the integrated stress response, which occurs in eukaryotic cells in response to accumulation of unfolded and misfolded proteins. Of note, results from siRNA-mediated knockdown of activating transcription factor 4 (ATF4) and overexpression of exogenous ATF4 cDNA indicated that ATF4 up-regulates *LAMP3* mRNA levels. Finally, ChIP assays verified an ATF4-binding site in the *LAMP3* gene promoter, and a dual-luciferase assay confirmed that this ATF4-binding site is indeed required for transcriptional up-regulation of *LAMP3*. These results reveal that ATF4 directly regulates *LAMP3*, representing the first identification of a gene for a lysosomal component whose expression is directly controlled by ATF4. This finding may provide a key link between stresses such as accumulation of unfolded proteins and modulation of autophagy, which removes them.

Lysosomes, the cellular sites of autophagy (the regulated destruction of cellular molecules and organelles), are recycled at a steady state in normal conditions. However, in response to cellular insults (such as accumulation of toxic products or nutrient depletion), there is an increase in the expression of lysosomal genes and in the numbers and size of lysosomes (1).

The transactivation of most lysosomal genes induced by cellular stress is mediated by transcription factor EB (TFEB)[3] (2, 3). A cohort of autophagy-related genes is also transactivated by TFEB during cellular stress (3), which further highlights the intricate link between autophagy and lysosomal biogenesis and function. Under basal conditions, TFEB resides in the cytoplasm in an inactive form. In more detail, mTOR complex 1 (mTORC1), a heteromeric protein kinase, which is activated by amino acids at the lysosomal surface, phosphorylates TFEB, thereby promoting its cytoplasmic retention and rendering it transcriptionally inactive. During cellular stress, mTORC1 activity is reduced and TFEB becomes dephosphorylated and can translocate to the nucleus, thus allowing it to drive the expression of its target genes (2, 4–9). The DNA sequence to which TFEB binds is known as the Coordinated Lysosomal Expression and Regulation (CLEAR) element, of which most lysosomal genes have at least one copy (1, 2).

However, there exists a subset of lysosomal genes with no evidence for regulation by TFEB, and the control of their expression during cellular stress remains relatively unstudied. The eukaryotic initiation factor (eIF) 2α/activating transcription factor (ATF) 4 pathway is central to the integrated stress response (ISR), a response to multiple stress stimuli that results in global changes in gene expression to either aid cell recovery or, if necessary, trigger apoptosis (10). For instance, the accumulation of unfolded proteins in the endoplasmic reticulum (ER) indirectly activates ATF4 through PKR-like endoplasmic reticulum kinase (PERK) (10, 11). PERK phosphorylates the α-subunit of eukaryotic initiation factor 2 (eIF2) thereby inhibiting the activity of eIF2's guanine nucleotide-exchange factor, eIF2B, and overall mRNA translation (11). However, the translation of some mRNAs, such as that encoding ATF4, is *enhanced* upon eIF2α phosphorylation. As the lysosome is an important site for degradation of misfolded protein during the

This work was supported by the Hopwood Centre for Neurobiology and by SAHMRI. The authors declare that they have no conflicts of interest with the contents of this article.

This article contains Figs. S1–S6 and Table S1.

[1] Both authors contributed equally to this work.

[2] To whom correspondence should be addressed: Lifelong Health Theme, South Australian Health and Medical Research Institute, P. O. Box 11060, Adelaide, South Australia 5001, Australia. Tel.: 61-8-8128-4923; E-mail: christopher.proud@sahmri.com.

[3] The abbreviations used are: TFEB, transcription factor EB; ATF4, activating transcription factor 4; ASNS, asparagine synthetase; BFA, brefeldin A; CHOP, CCAAT–enhancer-binding protein homologous protein; eIF2α, eukaryotic initiation factor 2α; ISR, integrated stress response; ISRIB, integrated stress response inhibitor; LAMP, lysosomal-associated membrane protein; mTOR, mammalian target of rapamycin; mTORC, mammalian target of rapamycin complex; PERK, PKR-like endoplasmic reticulum kinase; TPG, thapsigargin; TSS, transcriptional start site; UPR, unfolded protein response; qPCR, quantitative PCR; ER, endoplasmic reticulum; ANOVA, analysis of variance; ChIP-seq, ChIP sequencing.

Table 1
Oligonucleotides employed in this study for qPCR

Gene	Forward	Reverse
LAMP3 (NM_014398.3)	5′-taaaagcagagatggggatac-3′	5′-attttcgggtgccacagttc-3′
LITAF (NM_004862.3)	5′-gttgtccttcctgcaacaag-3′	5′-tgcagttgggacagtaatgg-3′
CHOP (NM_004083.5)	5′-cagctgagtcattgcctttc-3′	5′-ttgattcttcctcttcatttcc-3′
ATF4 (NM_001675.4) (42)	5′-ggccaagcacttcaaacctc-3′	5′-gagaaggcatcctccttgctg-3′
ASNS (NM_183356.3)	5′-gtggctctgttacaatggtg-3′	5′-gcagtatccagtaaaacaaatg-3′
XBP1 (NM_005080) (49)	5′-ccttgtagttgagaaccagg-3′	5′-ggggcttggtatatatgtgg-3′
LAMP1 (NM_005561.3)	5′-attgtgcgtcagcagcaatg-3′	5′-agcaccactgtggcatctg-3′
β-Actin	5′-ctggcaccacaccttctac-3′	5′-gggcacagtgtgggtgac-3′

unfolded protein response (UPR) (12, 13), we hypothesized that ATF4 might be involved in transcriptional regulation of non-TFEB–regulated lysosomal genes.

Lysosomal-associated membrane protein 3 (LAMP3) is a lysosomal membrane protein implicated in a range of cellular functions. For example, it is proposed to promote cardiac remodeling (14), is recruited to *Salmonella* to aid its intracellular proliferation (15), and contributes to protein degradation (16). Primarily, however, LAMP3 has been studied for its oncogenic properties. It is highly up-regulated in many forms of cancer, including osteosarcoma (17), breast cancer (18), and cervical cancer (19). Up-regulation of LAMP3 results in increased migration of breast cancer cells undergoing a hypoxia-driven UPR (20). High levels of LAMP3 in tumors during increased UPR have also been found to enhance radioresistance (the level of ionizing radiation a cell can withstand) in breast cancer cells. This was suggested to be a result of increased autophagy and increased DNA damage signaling and repair (21).

In this study, we demonstrate that transcription of the *LAMP3* gene is directly regulated by ATF4, and we verify the ATF4-binding site sequence. This is the first example of a lysosomal gene that is directly mediated by ATF4 binding upon cellular stress.

Results

Selection and qPCR screening of lysosomal genes not regulated by TFEB

To begin the investigation into lysosomal genes that are not regulated by TFEB, 16 genes were selected from the Human Lysosome Gene Database (22), on the basis that these genes had no CLEAR motif within 2000 bp upstream or downstream of the transcriptional start site (TSS) and no other evidence of regulation by TFEB. The genes chosen were as follows: *AGA, CREG1, CTBS, ENTPD4, GM2A, GNPTAB, LAMP2, LAMP3, LITAF, LMBRD1, NCSTN, OSTM1, PCYOX1, PPT2, SIAE,* and *TMEM92.*

Oligonucleotide primers overlapping adjacent exons were designed for each (Table 1 and Table S1), allowing for specific amplification of mRNA. Total RNA was then extracted from HeLa cells and used as a template for cDNA preparation and qualitative PCR, allowing for product size and specificity to be determined by gel electrophoresis prior to subsequent qPCR (data not shown).

To investigate the cellular stress-induced transactivation of these non-TFEB–regulated genes, human lung carcinoma A549 and cervical cancer HeLa cells were treated with brefeldin A (BFA), rapamycin, and the mTOR kinase inhibitor AZD8055 for 6 h and sucrose for 24 h. BFA induces the ISR by inhibiting ADP-ribosylation factors, leading to failure to recruit the Golgi membrane of coat protein β-COP (which acts as scaffold in the formation and budding of small membrane vesicles). This results in the collapse of the Golgi and its fusion with the ER, activating the UPR (23). Rapamycin inhibits mTORC1 by binding this complex together with the FK506-binding protein (24), thereby partially blocking its function. AZD8055 is an ATP-competitive inhibitor of both mTORC1 and mTORC2 (25). Sucrose induces lysosomal stress in HeLa and A549 cells (among others) due to both rapid uptake of sucrose into the lysosome, as well as the cells' inability to metabolize sucrose due to the absence of the enzyme invertase (26, 27). Sucrose treatment thus mimics the cellular pathology of lysosomal storage disorders, including TFEB activation and enhanced lysosomal biogenesis (2, 27). Collectively, these treatments allowed for an initial screening of the impact of the ISR, TFEB, and/or other mTORC1/2 controlled downstream effects or lysosomal stress on the regulation of each candidate gene. Ultimately, this indicated multiple classes of gene regulation; those regulated (potentially indirectly) by TFEB, the ISR, an unknown transcription factor, or by any combination of these (Figs. S1 and S2).

LAMP3 transcript levels increase upon BFA treatment

Total RNA was extracted from A549 and HeLa cells treated with BFA for 6 h, after which levels of transcript were analyzed by qPCR. CCAAT–enhancer-binding protein homologous protein (CHOP), a known target of ATF4 (28), was used as a positive control for induction of the ISR (Fig. 1). In response to BFA, appreciable increases were seen in the levels of *LAMP3* mRNA (3.29-fold in HeLa and 2.45-fold, compared with DMSO, in A549 cells), although they did not attain statistical significance ($p = 0.052$ and $p = 0.0698$, respectively) (Fig. 1). No significant or large magnitude changes in *LAMP3* mRNA were seen following treatment with either AZD8055 or rapamycin, supporting the conclusion that this lysosomal gene is not regulated through TFEB. In contrast, lipopolysaccharide-induced tumor necrosis factor (*LITAF*) did not appear to be regulated through either TFEB or the ISR, demonstrating that the regulation pattern seen for *LAMP3* is not shared by all genes for lysosomal proteins.

To then examine whether the effect of BFA on *LAMP3* mRNA levels was statistically significant and/or time-dependent, we examined *LAMP3* mRNA levels after 2, 4, 8, and 24 h of BFA treatment. In both HeLa and A549 cell lines, CHOP, a target for ATF4 and thus a positive control for activation of the ISR, was increased from 2 h onward, and *LAMP3* mRNA was

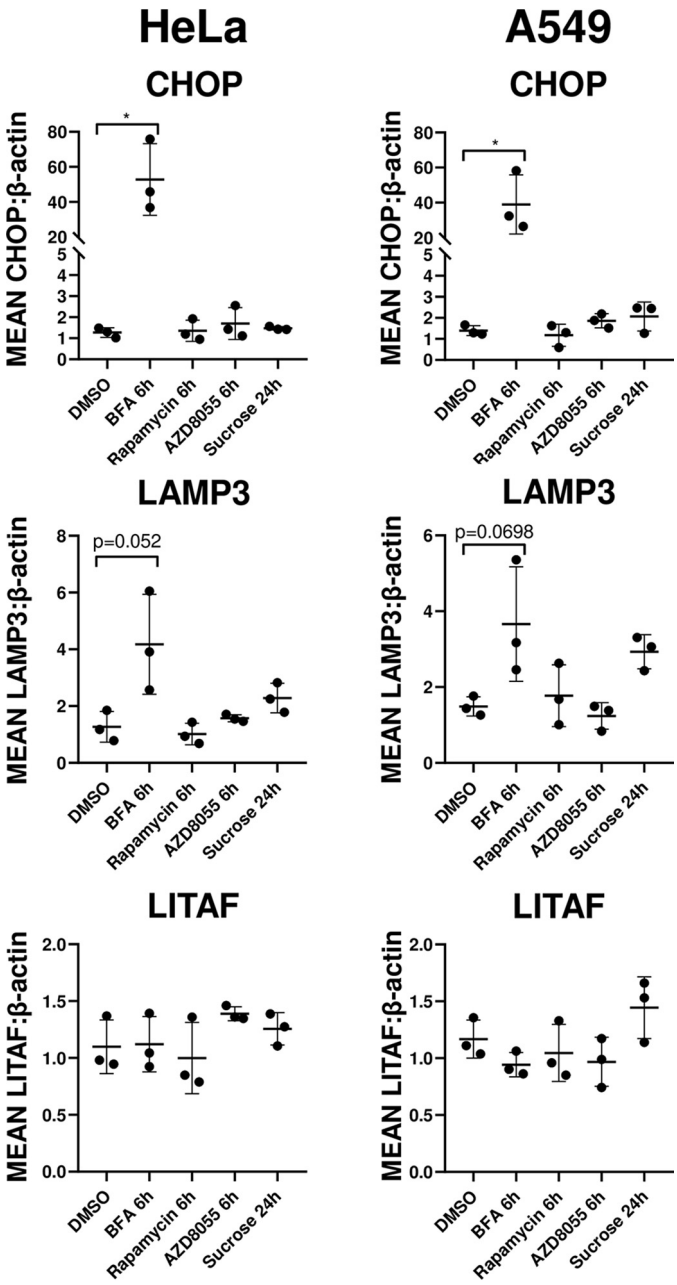

Figure 1. Effects of ER stress, mTORC1/2 inhibition, and lysosomal stress on the expression of selected genes in HeLa and A549 cell lines. Total RNA was extracted from HeLa or A549 cells that had been treated with 1:1000 DMSO, 5 μM BFA (6 h), 200 nM rapamycin (6 h), 1 μM AZD8055 (6 h), or 100 mM sucrose (24 h) and then used as a template for preparation of cDNA. cDNA samples were amplified and analyzed by qPCR using primers designed to amplify part of the coding sequence of the specified genes. Transcript levels were normalized to β-actin. Significance was calculated using Student's *t* test with mean for $n = 3$. *Error bars* represent $\pm$ S.D. For clarity, not all significant differences are indicated.

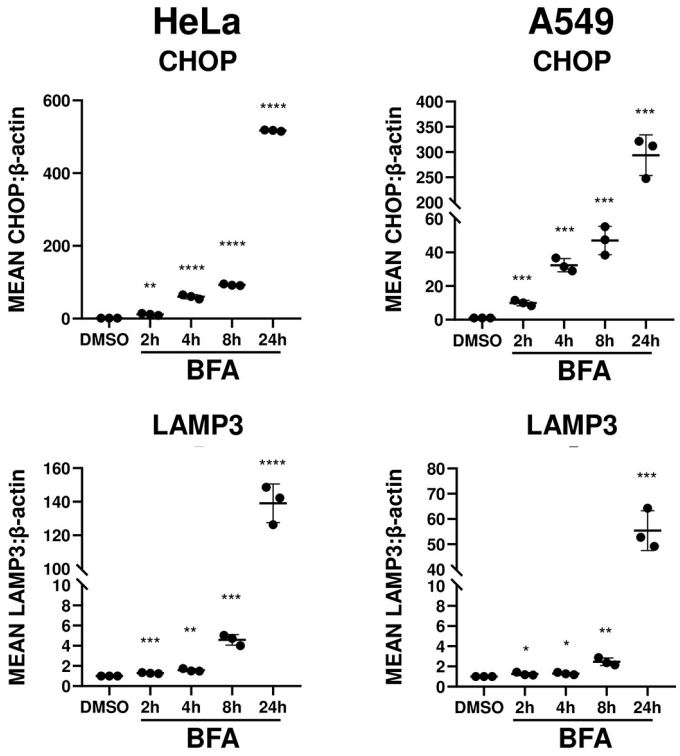

Figure 2. LAMP3 transcript levels increase with time in HeLa and A549 cells treated with BFA. Total RNA was extracted from HeLa or A549 cells that had been treated with 1:1000 DMSO for 24 h or 5 μM BFA for 2, 4, 8, and 24 h and then used as a template for preparation of cDNA. cDNA samples were amplified and analyzed by qPCR using primers designed to amplify the part of the coding sequence of the specified genes. Transcript levels were normalized to β-actin and presented as a fold-enrichment compared with the control (*DMSO*). Significance was calculated using Student's *t* test with mean for $n = 3$. *Error bars* represent $\pm$ S.D.

also significantly up-regulated at all time points tested (Fig. 2). Similar preliminary data were observed with the following three additional genes (Fig. S3): *CTBS*, *ENTPD4*, and *PPT2*.

Finally, to confirm that TFEB activation was incapable of up-regulating *LAMP3* mRNA, HeLa cells were transfected with a mammalian expression vector containing the cDNA for TFEB fused to the epitope for the FLAG antibody (2) or with empty vector, with or without subsequent treatment with AZD8055. Immunoblotting with antibodies to FLAG and TFEB phosphorylated on the mTORC1-regulated site at Ser-142 (pSer-142) collectively demonstrated the successful exogenous expression of TFEB, as well as the expected reduction in its phosphorylation upon treatment with AZD8055 (Fig. 3*A*). However, there was no detectable change in ATF4 protein subsequent to TFEB–FLAG expression and/or AZD8055 treatment. In addition, qPCR revealed that TFEB–FLAG caused a statistically significant increase in the mRNA levels for the known TFEB target *LAMP1*, which was, as anticipated, further increased by AZD8055 (Fig. 3*B*). In contrast, *LAMP3* expression was decreased upon TFEB–FLAG expression when compared with the control, regardless of the presence or absence of AZD8055 (Fig. 3*B*). These data provide strong further evidence that *LAMP3* is not a target of TFEB.

Implication of the phosphorylation of eIF2α in the regulation of LAMP3 transcription

The eIF2α/ATF4 pathway is central to the ISR. As mentioned above, the lysosome is an important site for degradation of misfolded protein during the UPR (12, 13), so we surmised that ATF4 might be involved in the transcriptional regulation of non-TFEB–regulated lysosomal genes, such as *LAMP3*.

To provide further evidence to support this idea, we employed compounds, in addition to BFA, that can promote eIF2α phosphorylation and downstream ATF4 activity. Thap-

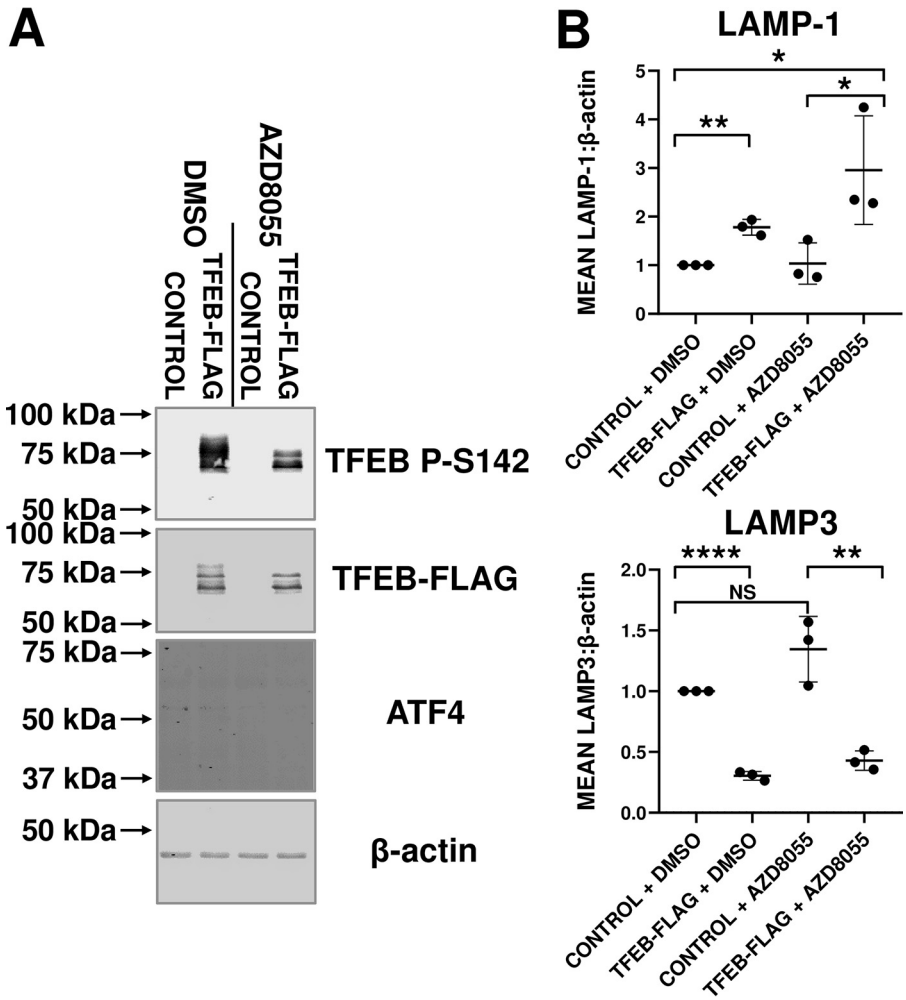

Figure 3. Increased TFEB activity does not increase *LAMP3* mRNA levels. *A,* HeLa cells were transfected with pTFEB–3xFLAG–CMV-10 or empty vector (*CONTROL*). Six h later, cells were treated with 1:1000 DMSO or 1 μM AZD8055. Twenty four h later, cells were lysed, and samples were analyzed via immunoblotting with the indicated antibodies ($n = 3$). *B,* total RNA was extracted from similarly-treated cells and then used as a template for preparation of cDNA. cDNA samples were amplified and analyzed by qPCR using primers designed to amplify part of the coding sequence of the specified genes. Transcript levels were normalized to β-actin and presented as a fold-enrichment compared with the control (*CONTROL + DMSO*). Significance was calculated using Student's *t* test with means for $n = 3$. *Error bars* represent ± S.D.

sigargin (TPG) promotes the ISR by inhibiting the transfer of Ca^{2+} ions into the ER (29). eIF2α can also be phosphorylated by general control nondepressible 2 (GCN2). Rather than responding to ER stress, GCN2 is activated upon amino acid starvation, which is signaled through the accumulation of uncharged tRNAs, resulting in stimulation of its protein kinase catalytic domain (30, 31). Histidinol inhibits the charging of histidyl-tRNA, and thus it activates the GCN2–eIF2α–ATF4 axis (32). In doing so, it mimics amino acid starvation, without eliciting the other direct consequences of amino acid depletion such as inhibition of mTORC1.

To assess whether TPG or histidinol treatments did indeed result in accumulation of ATF4 protein, A549 and HeLa cells were treated with each chemical for 24 h. Immunoblotting of extracts with antibodies directed to ATF4 demonstrated an increase in ATF4 protein expression in response to all three chemicals in both cell lines (Fig. 4*A*). To determine the effects of these agents on *LAMP3* transcript levels, total RNA was used as a template for cDNA preparation and subsequent analysis by qPCR. In both lines, in addition to BFA, TPG, and histidinol, each resulted in statistically-significant increases in both *LAMP3* mRNA, as well as the positive control, *CHOP* (Fig. 4*B*). However, the differences between the responses to these three different agents are noteworthy, particularly with respect to the lower ability of histidinol to up-regulate particularly *CHOP* and also (although to a lesser extent) *LAMP3* mRNA when compared with BFA and TPG. One reason for this is that components of the ISR, including ATF4, PERK, and CHOP, are also targets of the transcription factor XBP1, an additional mediator of the UPR whose activation is in turn regulated upon splicing of its message by IRE1 in the ER (33). Furthermore, ATF6 (the third arm of the UPR) has also been shown to induce expression of CHOP during ER stress (34). Indeed, in both HeLa and A549 cells, BFA and TPG, but not histidinol, caused an increase in BiP, an event that can occur due to the activation of any of the three arms of the UPR (Fig. S4*A*). This was further evidenced by the altered splicing of *XBP1* message (*i.e.* activation of XBP1) under these conditions (Fig. S4*B*). Therefore, BFA and TPG would be expected to cause a stronger ISR than histidinol. Nonetheless, these data demonstrate

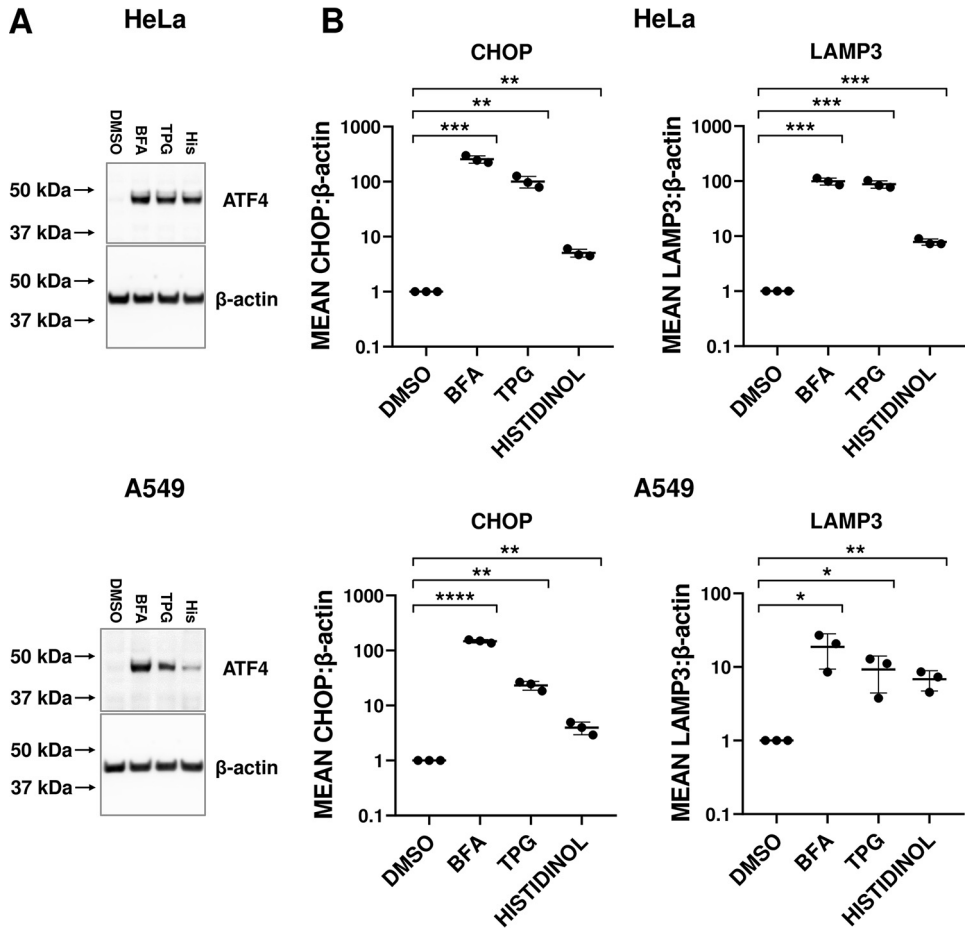

Figure 4. LAMP3 transcript levels are enhanced by additional chemical inducers of the ISR. *A,* HeLa and A549 cells were treated with 1:1000 DMSO, 5 μM BFA, 1 μM TPG, or 2 mM histidinol for 24 h. Extracts were then immunoblotted with antibodies to ATF4 and β-actin ($n = 3$). *B,* total RNA was extracted from similarly-treated cells and then used as a template for preparation of cDNA. cDNA samples were amplified and analyzed by qPCR using primers designed to amplify part of the coding sequence of the specified genes. Transcript levels were normalized to β-actin and presented as a fold-enrichment compared with the control (*DMSO*). Significance was calculated using Student's *t* test with mean for $n = 3$. *Error bars* represent $\pm$ S.D.

that multiple chemical inducers of ISR can up-regulate the transcript levels of *LAMP3*.

To further investigate the effect of eIF2α phosphorylation on specific genes, we used the compound ISRIB, which attenuates the inhibition of eIF2B caused by phosphorylated eIF2 (35) and thus allows assessment of the effect of eIF2α phosphorylation on gene regulation. To confirm that ISRIB inhibited the ISR in A549 and HeLa cells in our hands, each cell line was treated with BFA or BFA + ISRIB for 6 h, and extracts were then analyzed by immunoblotting. Both cell lines showed a marked induction of ATF4 protein expression in response to BFA, and as expected, this was reduced by ISRIB (Fig. 5*A*).

LAMP3 transcript levels were measured in response to treatment with BFA and/or ISRIB. HeLa and A549 cells were treated with BFA for 16 h, with or without pretreatment with ISRIB for 1 h. Total RNA was used as a template for cDNA preparation and subsequent analysis by qPCR. In each line, the 1-h pretreatment of ISRIB before a 16-h treatment with BFA resulted in a statistically-significant decrease in *LAMP3* mRNA levels, compared with just BFA treatment (Fig. 5*B*). This provides further evidence that, in A549 and HeLa cells, the regulation of *LAMP3* transcript levels involves the arm of the UPR that is mediated through phosphorylation of eIF2α. However, this was not the case for *CTBS*, *ENTPD4*, and *PPT2* (Fig. S5).

LAMP3 transactivation is perturbed by manipulating ATF4 expression

To determine the role of ATF4 itself (rather than any other component of the ISR) in regulating *LAMP3* mRNA levels, HeLa cells were transfected with either scrambled siRNA or one directed toward *ATF4* for 72 h, during the final 24 h of which the medium was supplemented with DMSO or BFA. Immunoblotting demonstrated a marked, statistically-significant decrease in BFA-induced levels of the ATF4 protein (Fig. 6, *A* and *B*) and mRNA (Fig. 6*C*) levels. Furthermore, we evaluated by qPCR the transcript levels of known direct ATF4 targets as well as *LAMP3* in identically-treated cells. Again, there was a drastic, statistically-significant decrease in both basal and BFA-induced *LAMP3* mRNA levels upon siRNA-mediated knockdown of *ATF4* (Fig. 6*C*). Interestingly, this was not the case with *CHOP*, although the levels of an additional known ATF4 target, asparagine synthetase (*ASNS*) (36), were reduced (Fig. 6*C*). In contrast, this was not the case for the three other putative targets of ATF4 (*CTBS*, *ENTPD4*, and *PPT2*) uncovered in our

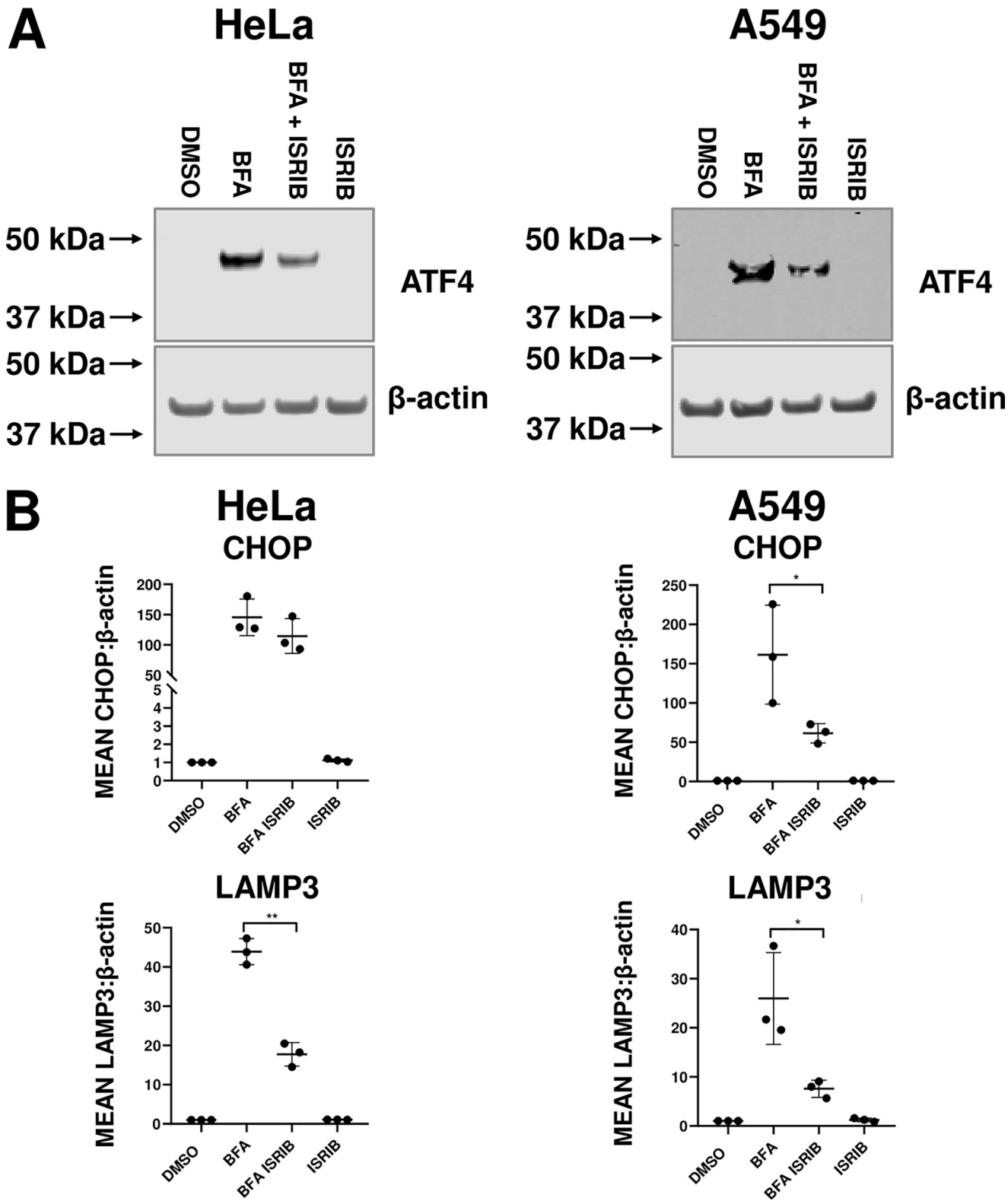

Figure 5. BFA-induced increases in *LAMP3* are attenuated by ISRIB. *A,* HeLa and A549 cells were treated with 1:1000 DMSO, 5 μM BFA (6 h), 5 μM BFA +200 nM ISRIB (6 h), or 200 nM ISRIB (6 h). Extracts were then immunoblotted with antibodies to ATF4 and β-actin ($n = 3$). *B,* total RNA was extracted from similarly-treated cells and then used as a template for preparation of cDNA. cDNA samples were amplified and analyzed by qPCR using primers designed to amplify part of the coding sequence of the specified genes. Transcript levels were normalized to β-actin and presented as a fold-enrichment compared with the control (*DMSO*). Significance was calculated using Student's *t* test with mean for $n = 3$. *Error bars* represent $\pm$ S.D. For clarity, not all the significant differences are indicated.

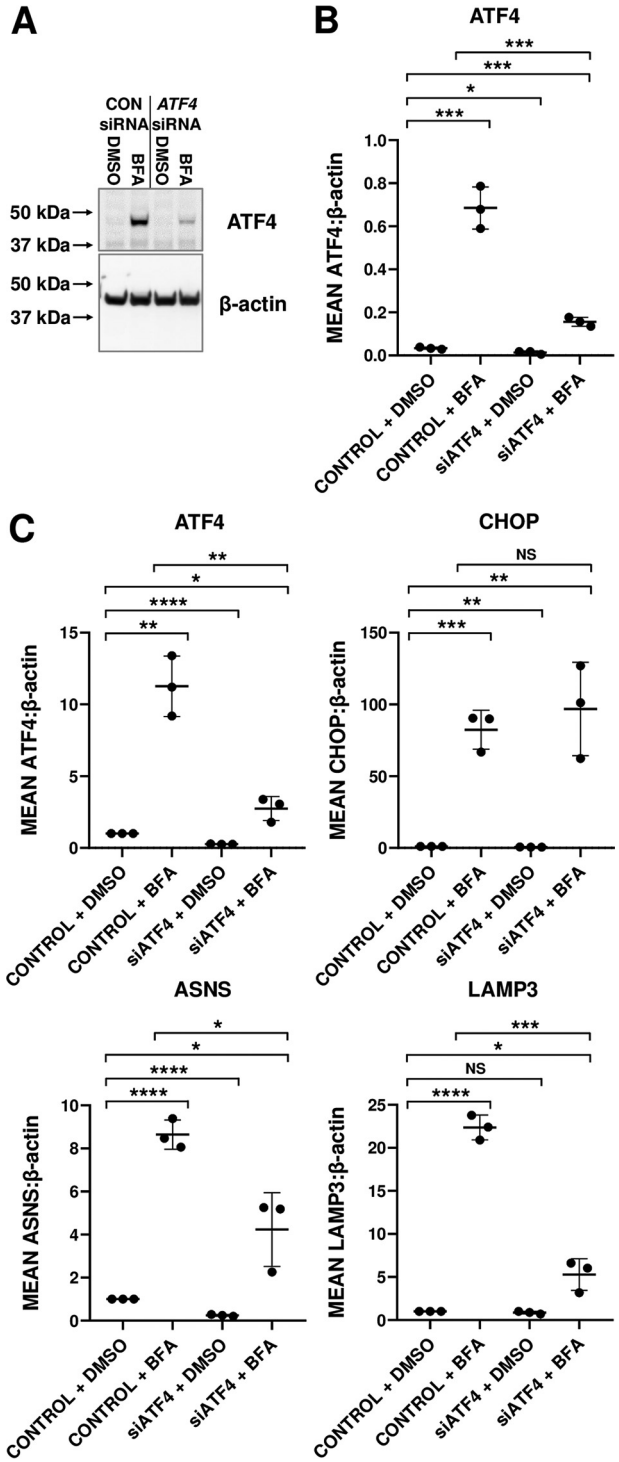

Figure 6. BFA-induced *LAMP3* expression is impaired upon siRNA-mediated *ATF4* knockdown. *A,* HeLa cells were transfected with 5 nM scrambled siRNA (*CONTROL*) or one directed toward *ATF4* (*siATF4*). After 48 h, cells were treated with 1:1000 DMSO or 5 μM BFA. 24 h later, cells were lysed, and samples were analyzed via immunoblotting with antibodies to ATF4 and β-actin ($n = 3$). *B,* ATF4 was quantified using densitometric analysis and normalized against β-actin, represented as the mean of the three biological replicates. *C,* total RNA was extracted from similarly-treated cells and then used as a template for preparation of cDNA. cDNA samples were amplified and analyzed by qPCR using primers designed to amplify part of the coding sequence of the specified genes. Transcript levels were normalized to β-actin and presented as a fold-enrichment compared with the control (*CONTROL* + *DMSO*). Significance was calculated using Student's *t* test with mean for $n = 3$. *Error bars* represent ± S.D.

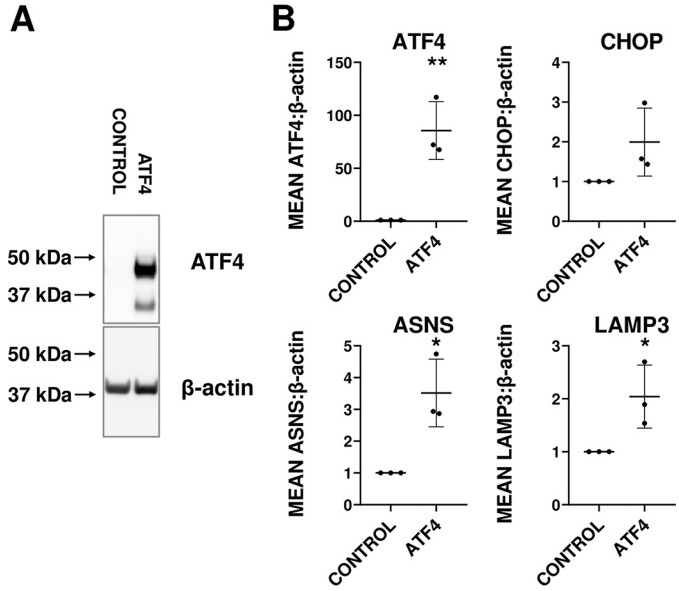

Figure 7. LAMP3 expression is up-regulated upon ATF4 overexpression under basal conditions. *A,* HeLa cells were transfected with pRK-ATF4 (*ATF4*) or empty vector (*CONTROL*). 24 h later, cells were lysed, and samples were analyzed via immunoblotting with antibodies to ATF4 and β-actin ($n = 3$). *B,* total RNA was extracted from similarly-treated cells and then used as a template for preparation of cDNA. cDNA samples were amplified and analyzed by qPCR using primers designed to amplify part of the coding sequence of the specified genes. Transcript levels were normalized to β-actin and presented as a fold-enrichment compared with the control (*DMSO*). Significance was calculated using Student's *t* test with mean for $n = 3$. *Error bars* represent ± S.D.

original screen (Fig. S6). Taken together, it is possible that these genes are not targets of ATF4 and/or their expression can also be mediated by other stress-inducible transcription factors (such as XBP1 or ATF6).

This indicates that ATF4 is required for the induction of *LAMP3* in response to BFA. To assess whether ATF4 suffices to drive its expression, we assessed the ability of exogenously expressed ATF4 to increase *LAMP3*. To that end, HeLa cells were transfected with a mammalian expression plasmid containing the cDNA for ATF4 or empty vector. After 24 h, immunoblotting or qPCR, respectively, demonstrated a substantial increase in ATF4 mRNA and protein when compared with the control (Fig. 7, *A* and *B*). Importantly, mRNA levels for *LAMP3* (and *ASNS*, the positive control) were up-regulated in a statistically significantly manner upon exogenous expression of ATF4 protein (Fig. 7*B*).

ATF4 associates with a binding site on LAMP3 upon BFA treatment

A collection of ChIP-seq data available from the Gene Transcription Regulation Database (37) revealed a potential ATF4-binding site within 1600 bp of the TSS of *LAMP3*, specifically ACATCTGATGCAAGGAAAA (reverse complement of TTTTCCTTGCATCAGATGT). The ATF4-binding consensus sequence has been reported as (G/A/C)TT(G/A/T)C(G/A)TCA (38), which matches the ChIP-seq data.

To investigate whether BFA induced the binding of ATF4 to this site, oligonucleotide primers were designed to flank this sequence near the *LAMP3* TSS, as well as a negative control (a region >1000 bp upstream of the site) (Table 2). The ATF4-

Table 2
Oligonucleotides employed in this study for ChIP

Gene	Region	Forward	Reverse
LAMP3 (NM_014398.3)	Positive	5′-tttaggaatgggagtcttggcttt-3′	5′-tgacactcttcctacacctttctg-3′
	Negative	5′-ggtagcacctggacagcaat-3′	5′-gggactggagggacaaacag-3′
ASNS (NM_183356)	Positive	5′-gcgctggaaacaaaagagct-3′	5′-taccgacctggctcctgtaa-3′
	Negative	5′-tgtagagctctggacggaca-3′	5′-gcccatttcccgtagcatct-3′

binding site involved in the regulation of *ASNS* was used as a positive control (36). HeLa cells were treated with DMSO or BFA for 6 h, prior to cross-linking of DNA and DNA-bound proteins with formaldehyde. Subsequent ChIP revealed significant binding of ATF4 near the TSS of *LAMP3* when comparing the BFA treatment to the DMSO control (Fig. 8).

BFA treatment increases the levels of a reporter, including the putative LAMP3 ATF4-binding site

The amplification after ChIP of a 118-bp segment of DNA near the *LAMP3* TSS confirmed the presence of an ATF4-binding site. To show conclusively that the site was involved in BFA-induced *LAMP3* up-regulation, the WT putative ATF4-binding site (termed "WT L3") was inserted into the firefly luciferase reporter plasmid pGL3-promoter (Promega) to determine the impact of the binding site on this reporter (Fig. 9*A*). In addition, two point mutations (MT1 L3 and MT2 L3) within the putative enhancer were separately introduced into the same reporter construct, in order to disrupt the consensus ATF4-binding sequence.

WT and mutant reporter plasmids were then transfected into HeLa cells. The reporter pRL-TK encoding *Renilla* luciferase was co-transfected as a control. In control cells (treated with DMSO), inclusion of WT L3 upstream of firefly luciferase results in a statistically significant 1.26-fold increase of firefly/*Renilla* luciferase expression, compared with the parent pGL3-promoter vector. This increase was not seen for vectors containing the mutated inserts (Fig. 9*B*). BFA induced statistically significant increases in firefly luciferase expression from the vector containing the WT L3 of 1.82-fold compared with pGL3-pro vector and 1.89-fold compared with the vector with the WT L3 insert after DMSO treatment. Importantly, these increases were not observed for the mutated inserts (Fig. 9*B*). Thus, BFA treatment induces firefly luciferase expression from a vector containing the WT L3 element, when ATF4 levels are enhanced, but not from mutant variants.

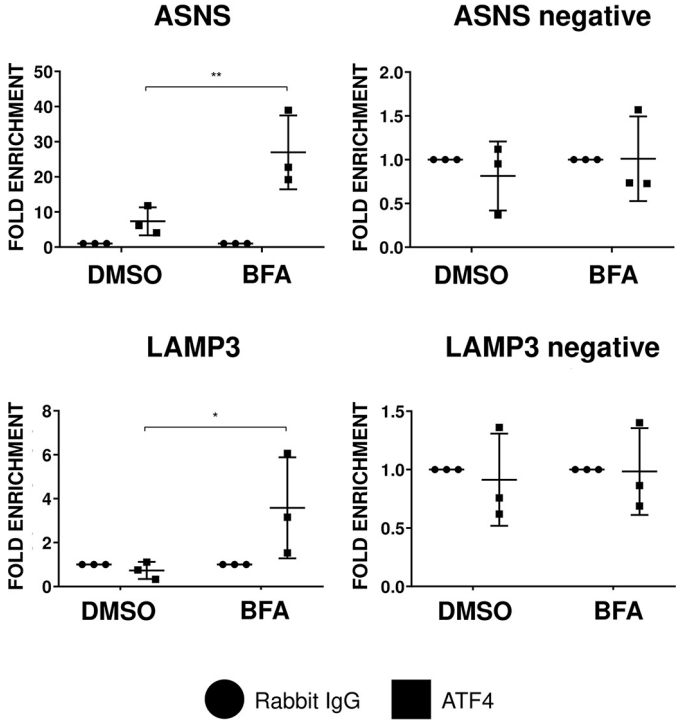

Figure 8. Verification of an ATF4-binding site near the TSS of *LAMP3*. HeLa cells were treated with 1:1000 DMSO and 5 μM BFA for 6 h, and then formaldehyde was used to cross-link DNA and protein. Samples were sonicated to shear chromatin, then immunoprecipitated with 1:200 ATF4 antibody or 1:500 normal rabbit IgG antibody. Chromatin was purified, then analyzed by qPCR in technical triplicates using primers designed to analyze known or potential ATF4-binding sites near the specified gene, as well as a region ~1000 bp upstream of each site (negative). Results are presented as a fold-enrichment of ATF4 *versus* normal rabbit IgG. DNA from the normal rabbit IgG was normalized to 1 for comparison with the ATF4 pulldown. Significance was calculated using two-way ANOVA with mean for $n = 3$. *Error bars* represent ± S.D.

Discussion

Since its discovery in 2009, TFEB has been established as a "master controller" of lysosomal biogenesis and function by regulating genes in the CLEAR network (1–3). However, there exists a subset of lysosomal and autophagy-associated genes with no evidence of regulation by TFEB. As also noted by others (39), a thorough understanding of the coordination of multiple nutrient-sensitive transcriptional pathways that coordinate gene expression of lysosomal genes is vital for a full understanding of lysosomal biogenesis. Our study has contributed to this goal by demonstrating the involvement of an additional stress-inducible transcription factor in the cellular stress up-regulation of lysosomal genes.

In this study, we focused on *LAMP3*, as levels of its mRNA were up-regulated in response to cellular stress induced by BFA (Figs. 1 and 2), but not by enhanced TFEB activity (Fig. 3). The use of alternative activators of the ISR (Fig. 4) and of ISRIB, an inhibitor of the ISR (Fig. 5), provided further supporting evidence that the phosphorylation of eIF2α results in up-regulation of *LAMP3*. Additionally, the siRNA-mediated knockdown of ATF4 (Fig. 6), as well as the overexpression of exogenous cDNA for ATF4 (Fig. 7), demonstrated a clear association between BFA-induced ATF4 activity and *LAMP3* mRNA levels. A search using the ChIP-seq database GTRD showed the presence of an unverified ATF4-binding site 1590 bp 3′ of the TSS of *LAMP3* (37); we confirmed that ATF4 binds the DNA within this region (Fig. 8). Finally, a 19-bp DNA segment containing the suspected ATF4-binding element (WT L3) was cloned into the multiple cloning region of the pGL3-promoter vector, as well as two mutant variants (Fig. 9*B*). When transfected into

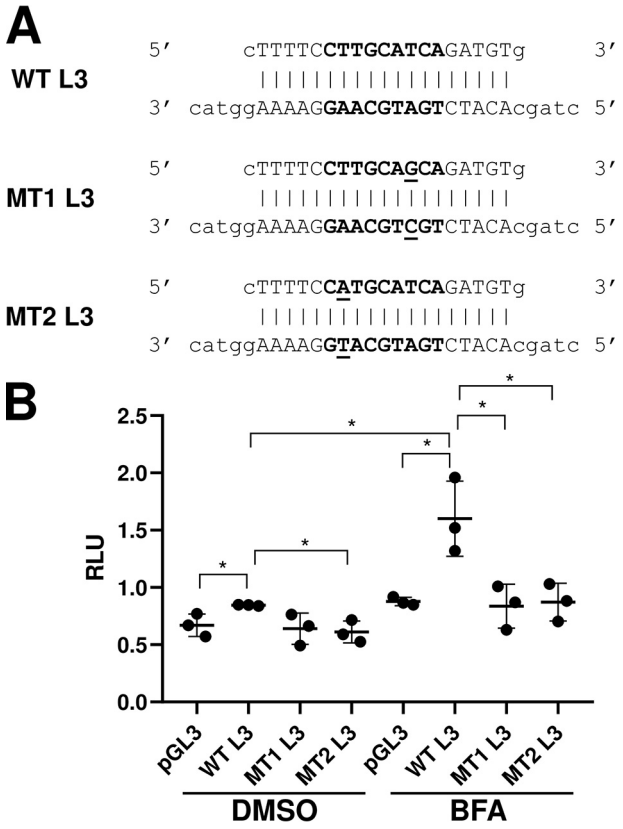

Figure 9. ATF4-binding site near the TSS of *LAMP3* mediates BFA-induced expression of a reporter. *A,* illustration of oligonucleotides designed for insertion into the pGL3-pro plasmid. *Boldface nucleotides* represent the putative ATF4-binding sequence (WT L3). *Underlined nucleotides* represent mutations introduced into the mutant variants (MT1 L3 and MT2 L3). *Lowercase* represents nucleotides chosen to allow for insertion into the KpnI/NheI-digested plasmid. *B,* HeLa cells were transfected with 50 ng of pRL-TK DNA and 50 ng of one of pGL3-pro, pGL3-pro + WT L3, pGL3-pro + MT1 L3, and pGL3-pro + MT2 L3, and then, 8 h later, were treated for 16 h with DMSO or BFA, as indicated. The Promega Dual-Glo luciferase assay system was then used to measure firefly and *Renilla* luciferase activity in each well. Results are presented as relative luciferase units (*RLU*) of firefly to *Renilla* luciferase activity. Significance was calculated using a Student's *t* test with mean for $n = 3$. *Error bars* represent ± S.D. For clarity, not all the significant differences are indicated.

HeLa cells, subsequent treatment with BFA caused a significant increase of reporter activity from the vector containing WT L3, which was in turn ablated by the presence of two mutations introduced into the binding site (Fig. 9*B*). Our collective data therefore show that *LAMP3* is a direct target of ATF4.

The PERK/ATF4 arm of the UPR has previously been implicated in the up-regulation of LAMP3 (21), and experiments with ATF4 siRNA illustrated that reduced ATF4 levels correlated with reduced *LAMP3* mRNA levels (in this case, in the context of an increase in *LAMP3* transcript mediated by inhibition of the proteasome) (16). However, those studies did not distinguish whether *LAMP3* is a direct target of ATF4 or an indirect one controlled by an additional transcription factor that is a direct target of ATF4 (such as CHOP (28)). Our results thus demonstrate that *LAMP3* is indeed a direct transcriptional target for ATF4. Furthermore, this is the first known example of a lysosomal gene being directly up-regulated by ATF4.

An additional point of interest arising from our observations is the apparent tight control of ATF4 over stress-induced *LAMP3* expression. The use of better-characterized direct targets of ATF4 is complicated by the influence of other factors in their transcriptional regulation. For instance, *CHOP* can also be a target for XBP1 and ATF6 (33, 34), explaining why levels of this mRNA enhanced by BFA treatment may not in turn be reduced by siRNA targeted toward ATF4 (Fig. 6). This leads us to suggest that *LAMP3* be adopted as a robust and thus preferentially chosen control when examining the effects of ATF4. However, it must be noted that the induction of reporter activity from the vector containing WT L3 upon BFA treatment containing the ATF4-binding element was quite small relative to the induction observed for the native gene. We therefore cannot categorically exclude the requirement for the binding of transcription factors to other important regulatory sequences in the *LAMP3* gene but that are absent from the artificial reporter, whether stress-induced (such as ATF6 or XBP1) or constitutive.

Autophagy is intricately linked with lysosomal biogenesis and function, and there are cohorts of nonlysosomal, autophagy-related genes that are transactivated by TFEB (3, 6), ATF4 (40), or both. For instance, the genes for the autophagosome cargo protein p62 (*SQSTM1*) (6, 40) and beclin-1 (*BECN1*), an initiator of autophagosome formation (2, 40), are direct targets of both TFEB and ATF4. *LAMP3* may be the first of several direct targets of ATF4 that encode genes for lysosomal proteins. However, similar to *SQSTM1* and *BECN1*, but not *LAMP3,* these are likely also to be transactivated by TFEB. This line of investigation could be pursued in future studies.

As the lysosome is an important site for the degradation of misfolded proteins (12, 13), it is logical that the ISR should mediate the cellular stress-induced up-regulation of lysosomal genes. Furthermore, some of the conditions that cause inactivation of mTORC1 (and thereby activate TFEB) can also promote the ISR. For instance, as mentioned above, in addition to ablating mTORC1 function, amino acid depletion also activates GCN2. Like PERK, this enzyme phosphorylates eIF2α and induces the ISR (10, 11). Moreover, there is evidence of regulatory cross-talk between TFEB and ATF4 (41, 42), although it must be noted that we saw no change in ATF4 protein levels in response to increased expression of TFEB (Fig. 3).

On an organellar level, it has recently been shown that CLN8, an ER-associated membrane protein whose deficiency results in the lysosomal storage disorder termed neuronal ceroid lipofuscinosis 8 (43), is necessary for the transport of lysosomal enzymes from the ER to the Golgi and through the endo-lysosomal system (44). Also, VAMP-associated proteins are known to mediate associations between the ER and Golgi; their deficiency ultimately leads to an increase in the number of endosomes, whose fusion with lysosomes in turn results in altered lysosomal pH and, presumably, dysfunction (45). In both cases, a deficiency in the ER is the actual cause of a lysosomal storage disorder, further demonstrating the pathophysiological links between ER stress and lysosomal stress, a connection that is becoming increasingly apparent and appreciated (13) and that is advanced by our work.

As mentioned previously, LAMP3 is proposed to contribute to several forms of cancer (17–21). Furthermore, in addition to the numerous known lysosomal storage disorders, lysosomal

and autophagic dysfunction has also been connected to neurological disorders, including Alzheimer's and Parkinson's diseases (46). Therefore, delineating the means by which *LAMP3* is regulated may contribute to developing strategies to counter its involvement in these diseases. In this study, we have extended understanding of the regulation of lysosomal genes and further expanded the association between ER stress, lysosomal biogenesis, and autophagy. This will likely contribute to research aimed at modulating these processes to treat disease.

Experimental procedures

Chemicals for cell treatments

AZD8055 (Selleck Chem), BFA (Sigma-Aldrich), rapamycin (Sigma-Aldrich), TPG (Sigma-Aldrich), and ISRIB (Sigma-Aldrich) were each dissolved in DMSO, whereas histidinol dihydrochloride (Sigma-Aldrich) and sucrose (Sigma-Aldrich) were prepared in Milli Q water.

Cell culture

A549 cells, derived from cancerous lung tissue, and HeLa cells, derived from cervical cancer cells, were maintained in Dulbecco's modified Eagle's medium with 10% (v/v) fetal bovine serum (Life Technologies, Inc.), 100 units/ml penicillin/streptomycin (Sigma-Aldrich) and incubated at 37 °C and 5% (v/v) CO_2. For experimentation, cells were plated either on 100-mm dishes (56.7 cm^2), 6-well plates (9.5 cm^2), or 96-well plates (0.32 cm^2). Cells were regularly tested for mycoplasma infection and discarded if affected.

Transient transfection

siRNAs to human *ATF4* (Qiagen), pRK-ATF4 (47), and pTFEB–3xFLAG–CMV-10 (2) were introduced into HeLa cells using Lipofectamine 3000 (Life Technologies, Inc.) according to the manufacturer's instructions. pRK-ATF4 was a gift from Yihong Ye (Addgene plasmid 26114; RRID: Addgene_26114).

RNA extraction

Cells grown in 6-well plates were washed using 2 ml of PBS, and then 500 μl of TRIzol reagent (Thermo Fisher Scientific) was added. Total RNA was subsequently prepared according to the manufacturer's instructions and provided a template for cDNA preparation.

Qualitative RT-PCR

cDNA was first prepared from total RNA using the SuperScript III First Strand Synthesis System (Life Technologies, Inc.). Oligonucleotide primers were designed to amplify fragments of the coding sequences of the genes of interest (Table 1). 50-μl samples were prepared using cDNA (prepared with 6.25 ng of starting RNA), 100 nM forward and reverse primer, 1 unit of HotStarTaq DNA polymerase, 1× Q-solution, 1 mM $MgCl_2$, 200 μM dNTP mix, and milliQ water. Reactions were performed at 95 °C for 15 min, 35 cycles of 94 °C for 1 min, 60 °C for 1 min, 72 °C for 1 min, and then 72 °C for 10 min. Products were electrophoresed through a 2% agarose gel and visualized by ethidium bromide staining on a Gel Doc XR apparatus (Bio-Rad).

Quantitative real-time PCR (qPCR)

cDNA was first prepared from total RNA using the SuperScript III First Strand Synthesis System (Life Technologies, Inc.). For each well, 0.84× FAST SYBR Green Mix (Applied Biosystems), 5–10 μl of cDNA (6.25–12.5 ng of starting RNA), 200 nM forward and reverse primer, and milliQ water to 20 μl were added. qPCRs proceeded as follows on an ABI Step One Plus qPCR instrument (Applied Biosystems): 95 °C for 20 s; 40× (95 °C for 3 s; 60 °C for 30 s). The comparative threshold cycle protocol was employed to determine amounts of the target mRNA.

Immunoblotting

Cells grown in 6-well plates were washed using 2 ml of ice-cold PBS, then lysed with 100–300 μl of RIPA buffer supplemented with 2.5 mM $Na_2H_2P_2O_7$ (Sigma-Aldrich), 1 mM β-glycerophosphate (Sigma-Aldrich), 1 mM Na_3VO_4 (Sigma-Aldrich), and 1× Protease Inhibitor Mixture (Roche Applied Science). Cells were then rocked for 30 min at 4 °C, scraped, and transferred to a microcentrifuge tube. Cell suspensions were centrifuged at 16,000 × *g* for 30 min at 4 °C, and then the supernatant was retained and transferred to new microcentrifuge tubes. Protein concentration was quantified for sample normalization via the Lowry assay (48).

Equal amounts (by protein) of samples were subjected to SDS-PAGE and then transferred to a nitrocellulose membrane. The membrane was blocked for ~90 min in PBS containing 0.1% Tween 20 and 2% (w/v) bovine serum albumin (BSA) at 4 °C. Membranes were then rolled overnight at 4 °C in the same solution supplemented with one of the following antibodies: 1:1000 rabbit monoclonal anti-ATF4 (Cell Signaling Technology); 1:1000 rabbit monoclonal anti-BiP (Cell Signaling Technology); 1:1500 mouse monoclonal anti-FLAG (Novus Biologicals); 1:1000 rabbit polyclonal anti-TFEB P-S142 (Millipore); or 1:10,000 mouse monoclonal anti-β-actin (Sigma-Aldrich). The following day, the membrane was washed three times for 5–10 min at room temperature in PBS containing 0.1% Tween 20, then rolled at room temperature for 1 h in PBS containing 0.1% Tween 20 and 2% BSA plus 1:20,000 goat anti-rabbit IgG DyLight 680 (Thermo Fisher Scientific) or goat anti-mouse IgG DyLight 800 4× PEG (Thermo Fisher Scientific) and imaged on an Odyssey CLx (LI-COR).

ChIP

Cells were grown for 2 days in 100-mm diameter dishes. To cross-link DNA and protein, cells were treated with 1% formaldehyde and rotated at room temperature for 10 min. Glycine was added at a final concentration of 125 mM, and samples were rotated for 5 min to quench the reaction. Cells were washed twice with PBS, scraped together with 0.5 ml of PBS + 1× protease inhibitor mixture into microcentrifuge tubes, and then pelleted by centrifugation at 4 °C at 1000 × *g* for 5 min. The supernatants were removed, and cells were resuspended and lysed for 10 min in 500 μl of ChIP lysis buffer (50 mM HEPES, pH 7.5, 140 mM NaCl, 1 mM EDTA, pH 8.0, 1% Triton X-100, 0.1% sodium deoxycholate, 0.1% SDS) + 1× protease inhibitor mixture at 4 °C. Sonication time was optimized as 300 s (in 30-s bursts, followed by 30 s to cool on ice) by gel

Table 3
***LAMP3* oligonucleotides employed in this study for luciferase reporter assays**

LAMP3	Upper	Lower
Wildtype (WT)	5′-cttttccttgcatcagatgtg-3′	5′-ctagcacatctgatgcaaggaaaaggtac-3′
Mutant 1 (MT1)	5′-cttttccttgcagcagatgtg-3′	5′-ctagcacatctgctgcaaggaaaaggtac-3′
Mutant 2 (MT2)	5′-cttttccatgcatcagatgtg-3′	5′-ctagcacatctgatgcatggaaaaggtac-3′

electrophoresis to ensure DNA fragment sizes of 150–900 bp. For analysis of sonicated samples created by ChIP, cell debris was pelleted by centrifugation for 10 min at 4 °C and 8000 × *g*. The supernatant was transferred into Eppendorf tubes and then diluted 1:2 with 500 μl of RIPA buffer. This sample was halved to allow probing with both ATF4 and normal rabbit IgG.

20 μl of suspended ChIP-grade protein G magnetic beads were added to each sample. Samples were then pre-cleared with 2 h of rotation at 4 °C. Samples were placed on a magnetic rack to pellet the beads, and solutions were isolated. 1% (5 μl) from each treatment/cell line was removed as an input control. Rabbit polyclonal ATF4 antibody (Cell Signaling Technology) was used at a 1:200 dilution, and 1 μl of normal rabbit IgG was added to one sample per cell line/treatment as a negative control. Samples were incubated for immunoprecipitation overnight at 4 °C with rotation. 20 μl of the protein G magnetic beads were then added to each sample for 2 h of incubation at 4 °C with rotation. The beads were pelleted, and the supernatant was discarded. The beads were washed with the addition of 1 ml of low-salt wash buffer and incubation at 4 °C three times at 5-min rotations, then repeated once using high-salt wash buffer. After the removal of the supernatant, DNA was eluted from beads with the addition of 150 μl of elution buffer per sample, including each specific 1% input sample. Chromatin was eluted by vortexing each sample at 1200 × *g* at 65 °C for 30 min. Beads were then pelleted, and chromatin samples were transferred to a new tube. Cross-linking was then reversed by addition of 6 μl of 5 M NaCl and 2 μl of proteinase K and vortexed at 1200 × *g* at 65 °C overnight.

DNA purification was achieved using the Qiagen QIAquick PCR purification kit and protocol, with elution in 50 μl of H_2O. In addition, primers were designed to flank this sequence near the *LAMP3* TSS, as well as a negative control region >1000 bp upstream of the site (negative control) (Table 2). DNA analysis was performed as per the previously mentioned qPCR method. In a 96-well plate, reactions contained 1 μl of purified DNA, 1× FAST SYBR Green Mix (Applied Biosystems), 200 nM forward and reverse primers, and Milli Q water to a total of 20 μl.

Construction of luciferase reporter plasmids

Oligonucleotides were annealed in 10-μl reactions containing 20 μM of the upper and lower strand oligonucleotides (Table 3), 1× T4 DNA Ligation Buffer, and 1 μl (10 units) of T4 polynucleotide kinase with Milli Q water. The solution was heated to 37 °C for 30 min, then to 95 °C for 5 min, and then cooled to 25 °C at a speed of 5 °C per min. These were then subcloned into KpnI- and NheI-digested pGL3-pro plasmid (Promega), which contains an SV40 promoter upstream of a luciferase gene, and fidelity was confirmed via sequencing.

Dual-luciferase reporter assay

HeLa cells were grown in 96-well plates. 50 ng of pGL3-pro plasmid with or without the WT or mutated ATF4-binding sites of *LAMP3*, as well as 50 ng of pRL-TK (Promega), were transfected using Lipofectamine 3000 according to the manufacturer's instructions (Thermo Fisher Scientific). The cells were incubated for 8 h before removal of transfection reagents and addition of chemicals for testing.

Luciferase assays were performed using the Dual-Glo Luciferase Assay System (Promega). Upon completion of treatments, 50 μl of Dual-Glo reagent was added to each well, and then samples were incubated at room temperature for 15 min. The firefly luciferase luminescence was recorded using a GloMax Discover Microplate Reader with an integration time of 0.3 s. An equivalent volume of Dual-Glo "Stop & Glo" reagent was then added, and again incubated at room temperature for 15 min before recording of *Renilla* luminescence. To determine activity of each promoter site, the firefly:*Renilla* luminescence ratio was calculated.

Statistics

For immunoblotting and qualitative RT-PCR, experiments were performed in biological triplicate. For qPCR, experiments were performed in biological triplicate, with each replicate analyzed in turn in technical triplicate. Statistical significance was performed using the Student's *t* test and two-way ANOVA. Error bars represent ± standard deviation (S.D.). * = $p \leq 0.05$, ** = $p \leq 0.01$, *** = $p \leq 0.001$, and **** = $p \leq 0.001$.

Data availability

The data used and/or analyzed during the current study are contained within the text or available from the corresponding author on reasonable request.

Author contributions—T. D. B. and A. O. F. data curation; T. D. B. and A. O. F. formal analysis; T. D. B., A. O. F., J. X., and L. Y. S. validation; T. D. B., A. O. F., J. X., and L. Y. S. investigation; T. D. B., A. O. F., J. X., and L. Y. S. visualization; T. D. B., A. O. F., and C. G. P. writing-original draft; A. O. F. conceptualization; A. O. F. and C. G. P. supervision; A. O. F. and C. G. P. project administration; A. O. F. and C. G. P. writing-review and editing; C. G. P. resources; C. G. P. funding acquisition.

Acknowledgments—We are grateful to James Merrett (Lifelong Health Theme, SAHMRI), who helped design the ChIP experiments; Stuart De Poi (Lifelong Health Theme, SAHMRI), for assistance in plasmid transfections; Prof. Andrea Ballabio (Telethon Institute of Genetics and Medicine, Naples, Italy) for the kind gift of pTFEB–3xFLAG–CMV-10.

References

1. Ballabio, A. (2016) The awesome lysosome. *EMBO. Mol. Med.* **8,** 73–76 CrossRef Medline
2. Sardiello, M., Palmieri, M., di Ronza, A., Medina, D. L., Valenza, M., Gennarino, V. A., Di Malta, C., Donaudy, F., Embrione, V., Polishchuk, R. S., Banfi, S., Parenti, G., Cattaneo, E., and Ballabio, A. (2009) A gene network regulating lysosomal biogenesis and function. *Science* **325,** 473–477 CrossRef Medline
3. Palmieri, M., Impey, S., Kang, H., di Ronza, A., Pelz, C., Sardiello, M., and Ballabio, A. (2011) Characterization of the CLEAR network reveals an integrated control of cellular clearance pathways. *Hum. Mol. Genet.* **20,** 3852–3866 CrossRef Medline
4. Settembre, C., Zoncu, R., Medina, D. L., Vetrini, F., Erdin, S., Erdin, S., Huynh, T., Ferron, M., Karsenty, G., Vellard, M. C., Facchinetti, V., Sabatini, D. M., and Ballabio, A. (2012) A lysosome-to-nucleus signaling mechanism senses and regulates the lysosome via mTOR and TFEB. *EMBO J.* **31,** 1095–1108 CrossRef Medline
5. Roczniak-Ferguson, A., Petit, C. S., Froehlich, F., Qian, S., Ky, J., Angarola, B., Walther, T. C., and Ferguson, S. M. (2012) The transcription factor TFEB links mTORC1 signaling to transcriptional control of lysosome homeostasis. *Sci. Signal.* **5,** ra42 CrossRef Medline
6. Settembre, C., Di Malta, C., Polito, V. A., Garcia Arencibia, M., Vetrini, F., Erdin, S., Erdin, S. U., Huynh, T., Medina, D., Colella, P., Sardiello, M., Rubinsztein, D. C., and Ballabio, A. (2011) TFEB links autophagy to lysosomal biogenesis. *Science* **332,** 1429–1433 CrossRef Medline
7. Peña-Llopis, S., Vega-Rubin-de-Celis, S., Schwartz, J. C., Wolff, N. C., Tran, T. A., Zou, L., Xie, X. J., Corey, D. R., and Brugarolas, J. (2011) Regulation of TFEB and V-ATPases by mTORC1. *EMBO J.* **30,** 3242–3258 CrossRef Medline
8. Martina, J. A., Chen, Y., Gucek, M., and Puertollano, R. (2012) MTORC1 functions as a transcriptional regulator of autophagy by preventing nuclear transport of TFEB. *Autophagy* **8,** 903–914 CrossRef Medline
9. Martina, J. A., and Puertollano, R. (2013) Rag GTPases mediate amino acid-dependent recruitment of TFEB and MITF to lysosomes. *J. Cell Biol.* **200,** 475–491 CrossRef Medline
10. Pakos-Zebrucka, K., Koryga, I., Mnich, K., Ljujic, M., Samali, A., and Gorman, A. M. (2016) The integrated stress response. *EMBO Rep.* **17,** 1374–1395 CrossRef Medline
11. Pavitt, G. D. (2018) Regulation of translation initiation factor eIF2B at the hub of the integrated stress response. *Wiley Interdiscip. Rev. RNA* **9,** e1491 CrossRef Medline
12. Jackson, M. P., and Hewitt, E. W. (2016) Cellular proteostasis: degradation of misfolded proteins by lysosomes. *Essays Biochem.* **60,** 173–180 CrossRef Medline
13. De Leonibus, C., Cinque, L., and Settembre, C. (2019) Emerging lysosomal pathways for quality control at the endoplasmic reticulum. *FEBS Lett.* **593,** 2319–2329 CrossRef Medline
14. Jiang, D. S., Yi, X., Huo, B., Liu, X. X., Li, R., Zhu, X. H., and Wei, X. (2016) The potential role of lysosome-associated membrane protein 3 (LAMP3) on cardiac remodeling. *Am. J. Transl. Res.* **8,** 37–48 Medline
15. Lee, E. J., Park, K. S., Jeon, I. S., Choi, J. W., Lee, S. J., Choy, H. E., Song, K. D., Lee, H. K., and Choi, J. K. (2016) LAMP-3 (Lysosome-Associated Membrane Protein 3) promotes the intracellular proliferation of *Salmonella typhimurium*. *Mol. Cells* **39,** 566–572 CrossRef Medline
16. Dominguez-Bautista, J. A., Klinkenberg, M., Brehm, N., Subramaniam, M., Kern, B., Roeper, J., Auburger, G., and Jendrach, M. (2015) Loss of lysosome-associated membrane protein 3 (LAMP3) enhances cellular vulnerability against proteasomal inhibition. *Eur. J. Cell Biol.* **94,** 148–161 CrossRef Medline
17. Liu, S., Yue, J., Du, W., Han, J., and Zhang, W. (2018) LAMP3 plays an oncogenic role in osteosarcoma cells partially by inhibiting TP53. *Cell. Mol. Biol. Lett.* **23,** 33 CrossRef Medline
18. Nagelkerke, A., Mujcic, H., Bussink, J., Wouters, B. G., van Laarhoven, H. W., Sweep, F. C., and Span, P. N. (2011) Hypoxic regulation and prognostic value of LAMP3 expression in breast cancer. *Cancer* **117,** 3670–3681 CrossRef Medline
19. Kanao, H., Enomoto, T., Kimura, T., Fujita, M., Nakashima, R., Ueda, Y., Ueno, Y., Miyatake, T., Yoshizaki, T., Buzard, G. S., Tanigami, A., Yoshino, K., and Murata, Y. (2005) Overexpression of LAMP3/TSC403/DC-LAMP promotes metastasis in uterine cervical cancer. *Cancer Res.* **65,** 8640–8645 CrossRef Medline
20. Nagelkerke, A., Bussink, J., Mujcic, H., Wouters, B. G., Lehmann, S., Sweep, F. C., and Span, P. N. (2013) Hypoxia stimulates migration of breast cancer cells via the PERK/ATF4/LAMP3-arm of the unfolded protein response. *Breast Cancer Res.* **15,** R2 CrossRef Medline
21. Nagelkerke, A., Bussink, J., van der Kogel, A. J., Sweep, F. C., and Span, P. N. (2013) The PERK/ATF4/LAMP3-arm of the unfolded protein response affects radioresistance by interfering with the DNA damage response. *Radiother. Oncol.* **108,** 415–421 CrossRef Medline
22. Brozzi, A., Urbanelli, L., Germain, P. L., Magini, A., and Emiliani, C. (2013) hLGDB: a database of human lysosomal genes and their regulation. *Database* **2013,** bat024 CrossRef Medline
23. Chardin, P., and McCormick, F. (1999) Brefeldin A: the advantage of being uncompetitive. *Cell* **97,** 153–155 CrossRef Medline
24. Li, J., Kim, S. G., and Blenis, J. (2014) Rapamycin: one drug, many effects. *Cell Metab.* **19,** 373–379 CrossRef Medline
25. Chresta, C. M., Davies, B. R., Hickson, I., Harding, T., Cosulich, S., Critchlow, S. E., Vincent, J. P., Ellston, R., Jones, D., Sini, P., James, D., Howard, Z., Dudley, P., Hughes, G., Smith, L., *et al.* (2010) AZD8055 is a potent, selective, and orally bioavailable ATP-competitive mammalian target of rapamycin kinase inhibitor with *in vitro* and *in vivo* antitumor activity. *Cancer Res.* **70,** 288–298 CrossRef Medline
26. Kato, T., Okada, S., Yutaka, T., and Yabuuchi, H. (1984) The effects of sucrose loading on lysosomal hydrolases. *Mol. Cell. Biochem.* **60,** 83–98 CrossRef Medline
27. Karageorgos, L. E., Isaac, E. L., Brooks, D. A., Ravenscroft, E. M., Davey, R., Hopwood, J. J., and Meikle, P. J. (1997) Lysosomal biogenesis in lysosomal storage disorders. *Exp. Cell Res.* **234,** 85–97 CrossRef Medline
28. Averous, J., Bruhat, A., Jousse, C., Carraro, V., Thiel, G., and Fafournoux, P. (2004) Induction of CHOP expression by amino acid limitation requires both ATF4 expression and ATF2 phosphorylation. *J. Biol. Chem.* **279,** 5288–5297 CrossRef Medline
29. Sano, R., and Reed, J. C. (2013) ER stress-induced cell death mechanisms. *Biochim. Biophys. Acta* **1833,** 3460–3470 CrossRef Medline
30. Dong, J., Qiu, H., Garcia-Barrio, M., Anderson, J., and Hinnebusch, A. G. (2000) Uncharged tRNA activates GCN2 by displacing the protein kinase moiety from a bipartite tRNA-binding domain. *Mol. Cell* **6,** 269–279 CrossRef Medline
31. Zhang, P., McGrath, B. C., Reinert, J., Olsen, D. S., Lei, L., Gill, S., Wek, S. A., Vattem, K. M., Wek, R. C., Kimball, S. R., Jefferson, L. S., and Cavener, D. R. (2002) The GCN2 eIF2α kinase is required for adaptation to amino acid deprivation in mice. *Mol. Cell. Biol.* **22,** 6681–6688 CrossRef Medline
32. Hansen, B. S., Vaughan, M. H., and Wang, L. (1972) Reversible inhibition by histidinol of protein synthesis in human cells at the activation of histidine. *J. Biol. Chem.* **247,** 3854–3857 Medline
33. Acosta-Alvear, D., Zhou, Y., Blais, A., Tsikitis, M., Lents, N. H., Arias, C., Lennon, C. J., Kluger, Y., and Dynlacht, B. D. (2007) XBP1 controls diverse cell type- and condition-specific transcriptional regulatory networks. *Mol. Cell* **27,** 53–66 CrossRef Medline
34. Yoshida, H., Okada, T., Haze, K., Yanagi, H., Yura, T., Negishi, M., and Mori, K. (2000) ATF6 activated by proteolysis binds in the presence of NF-Y (CBF) directly to the cis-acting element responsible for the mammalian unfolded protein response. *Mol. Cell. Biol.* **20,** 6755–6767 CrossRef Medline
35. Zyryanova, A. F., Weis, F., Faille, A., Alard, A. A., Crespillo-Casado, A., Sekine, Y., Harding, H. P., Allen, F., Parts, L., Fromont, C., Fischer, P. M., Warren, A. J., and Ron, D. (2018) Binding of ISRIB reveals a regulatory site in the nucleotide exchange factor eIF2B. *Science* **359,** 1533–1536 CrossRef Medline
36. Shan, J., Ord, D., Ord, T., and Kilberg, M. S. (2009) Elevated ATF4 expression, in the absence of other signals, is sufficient for transcriptional induction via CCAAT enhancer-binding protein-activating transcription factor response elements. *J. Biol. Chem.* **284,** 21241–21248 CrossRef Medline

37. Yevshin, I., Sharipov, R., Kolmykov, S., Kondrakhin, Y., and Kolpakov, F. (2019) GTRD: a database on gene transcription regulation–2019 update. *Nucleic Acids Res.* **47,** D100–D105 CrossRef Medline
38. Marchand, A., Tomkiewicz, C., Magne, L., Barouki, R., and Garlatti, M. (2006) Endoplasmic reticulum stress induction of insulin-like growth factor-binding protein-1 involves ATF4. *J. Biol. Chem.* **281,** 19124–19133 CrossRef Medline
39. Lamming, D. W., and Bar-Peled, L. (2019) Lysosome: the metabolic signaling hub. *Traffic* **20,** 27–38 CrossRef Medline
40. B'chir, W., Maurin, A. C., Carraro, V., Averous, J., Jousse, C., Muranishi, Y., Parry, L., Stepien, G., Fafournoux, P., and Bruhat, A. (2013) The eIF2α/ATF4 pathway is essential for stress-induced autophagy gene expression. *Nucleic Acids Res.* **41,** 7683–7699 CrossRef Medline
41. Martina, J. A., Diab, H. I., Brady, O. A., and Puertollano, R. (2016) TFEB and TFE3 are novel components of the integrated stress response. *EMBO J.* **35,** 479–495 CrossRef Medline
42. Park, Y., Reyna-Neyra, A., Philippe, L., and Thoreen, C. C. (2017) mTORC1 balances cellular amino acid supply with demand for protein synthesis through post-transcriptional control of ATF4. *Cell Rep.* **19,** 1083–1090 CrossRef Medline
43. Ranta, S., Zhang, Y., Ross, B., Lonka, L., Takkunen, E., Messer, A., Sharp, J., Wheeler, R., Kusumi, K., Mole, S., Liu, W., Soares, M. B., Bonaldo, M. F., Hirvasniemi, A., de la Chapelle, A., Gilliam, T. C., and Lehesjoki, A. E. (1999) The neuronal ceroid lipofuscinoses in human EPMR and *mnd* mutant mice are associated with mutations in *CLN8*. *Nat. Genet.* **23,** 233–236 CrossRef Medline
44. di Ronza, A., Bajaj, L., Sharma, J., Sanagasetti, D., Lotfi, P., Adamski, C. J., Collette, J., Palmieri, M., Amawi, A., Popp, L., Chang, K. T., Meschini, M. C., Leung, H. E., Segatori, L., Simonati, A., *et al.* (2018) CLN8 is an endoplasmic reticulum cargo receptor that regulates lysosome biogenesis. *Nat. Cell Biol.* **20,** 1370–1377 CrossRef Medline
45. Mao, D., Lin, G., Tepe, B., Zuo, Z., Tan, K. L., Senturk, M., Zhang, S., Arenkiel, B. R., Sardiello, M., and Bellen, H. J. (2019) VAMP associated proteins are required for autophagic and lysosomal degradation by promoting a PtdIns4P-mediated endosomal pathway. *Autophagy* **15,** 1214–1233 CrossRef Medline
46. Levine, B., and Kroemer, G. (2019) Biological functions of autophagy genes: a disease Perspective. *Cell* **176,** 11–42 CrossRef Medline
47. Wang, Q., Mora-Jensen, H., Weniger, M. A., Perez-Galan, P., Wolford, C., Hai, T., Ron, D., Chen, W., Trenkle, W., Wiestner, A., and Ye, Y. (2009) ERAD inhibitors integrate ER stress with an epigenetic mechanism to activate BH3-only protein NOXA in cancer cells. *Proc. Natl. Acad. Sci. U.S.A.* **106,** 2200–2205 CrossRef Medline
48. Lowry, O. H., Rosebrough, N. J., Farr, L., and Randall, R. J. (1951) Protein measurement with the Folin phenol reagent. *J. Biol. Chem.* **193,** 265–275 Medline
49. Yoshida, H., Matsui, T., Yamamoto, A., Okada, T., and Mori, K. (2001) XBP1 mRNA is induced by ATF6 and spliced by IRE1 in response to ER stress to produce a highly active transcription factor. *Cell* **107,** 881–891 CrossRef Medline